Journal of Sound and Vibration (1999) **226**(1), 149–167
Article No. jsvi.1999.2286, available online at http://www.idealibrary.com on IDEAL®

EXTENSION OF MODAL ANALYSIS TO LINEAR TIME-VARYING SYSTEMS

KEFU LIU

Department of Mechanical Engineering, Lakehead University, Thunder Bay, Ontario, Canada P7B 5E1

(*Received* 8 *September* 1998, *and in final form* 31 *March* 1999)

Linear time-varying (LTV) systems have been often dealt with on a case-by-case basis. Many well-developed concepts and analytic methods of linear time-invariant (LTI) systems cannot be applied to LTV systems. For example, the conventional definition of modal parameters is invalid for LTV systems. The first part of this paper explores the possibility of extending the modal concept of LTV systems. The discrete-time state-space model is used to represent LTV systems. By analogy to LTI systems, the pseudo-modal parameters are defined using the eigenvalues of the discrete-time state transition matrix. The paper shows that the pseudo-modal parameters preserve certain properties of the conventional modal parameters defined for LTI systems. The second part of the paper extends a previously developed algorithm to identify the pseudo-modal parameters using forced responses and forcing inputs. For a general LTV system, the input and output Hankel matrices formed by an ensemble of data satisfy a matrix facotrization relation. The key step of the method is to modify the output matrix in such a way that the range space of the observability matrix can be extracted. A robotic manipulator with varying inertia links is used as an example. The first part of the numerical simulation illustrates the applications of the pseudo-modal parameters. The second part of the simulation tests the identification algorithm under different conditions. Several practical issues are addressed.

1. INTRODUCTION

Modal parameters including natural frequencies and modal damping ratios describe the global properties of linear time-invariant (LTI) systems. These parameters have been widely used to characterize LTI systems [1]. It has been desired to extend modal concepts to linear time-varying (LTV) systems. However, LTV systems violate one of the assumptions of the conventional modal analysis, that is, stationarity. Some attempts in this direction have been made. Zadeh [2, 3] defined the time-varying transfer function by extending the Laplace transform to the varying impulsive response. However, in general, no closed-form of the Zadeh's transfer function is known. Furthermore, the use of the Zadeh's transfer function in a limited-time variation seems problematic since the definition assumes that the variation continues infinitely. The singularity or varying pole of the Zadeh's

0022-460X/99/360149 + 19 $30.00/0

transfer function was used to study the stability of time-varying systems [4]. Again, finding those varying poles is extremely difficult or impossible in most times. On the other hand, 'varying eigenvalues' or 'varying natural frequencies' have been used without a rigorous definition [5–8]. The concept of the pseudo-modal parameters was introduced in a previous study [9]. The pseudo-modal parameters are related to the eigenvalues of the varying discrete-time state transition matrices by analogy to LTI systems. The pseudo-modal parameters offer a solution to describe dynamic properties of LTV systems using a compact set of parameters. The applicability of the pseudo-modal parameters deserves a further investigation.

Many attempts have been made to address identification of LTV systems. Some early efforts simply extended standard time-invariant methods to a short data segment from a LTV system under the assumption that the system dynamics does not change significantly in this period [10]. The use of adaptive methods recognized that the model representing a LTV system should be time-dependent as well. For example, if the system variation is slow, the coefficients of an autoregressive, moving average (ARMA) model can be assumed to be time-dependent and the evolution of the coefficients can be tracked by adaptive algorithms [11, 12]. To further improve tracking ability, the parameters of the ARMA model can be represented by time functions with a known structure, such as a polynomial function. This way, the identification problem is equivalent to estimating the coefficients of the polynomial functions [13]. A common feature of the afore-mentioned methods is the use of data form a single experiment. Ensemble methods are different approaches that use a series of input and output data from multiple experiments on the system undergoing the same variation. Because the dynamic behaviors of the system at each moment are represented by an ensemble of input and output data, many standard time-invariant methods can be readily extended to LTV systems [14, 15]. The ensemble methods require no *a priori* knowledge of the variation form of system parameters and are not limited by the parameter variability. In a previous study [9], an algorithm to identify the pseudo-modal parameters was developed. The algorithm is based on the ensemble methods and subspace extraction schemes [16]. However, the algorithm is limited to the use of free responses.

Two main objectives of this study are: to further explore the applicability of the pseudo-modal parameters for LTV systems and to extend the algorithm proposed in reference [9] to the case of using forced responses and forcing inputs. The paper is organized as follows. Section 2 addresses characterization of LTV systems using the pseudo-modal parameters. Section 3 develops an algorithm for the identification of the pseudo-modal parameters. Section 4 presents an illustrative example to show the application of the pseudo-modal parameters and test the proposed identification algorithm.

2. CHARACTERIZATION OF DYNAMICS OF LTV SYSTEMS

An n-degree-of-freedom (d.o.f) LTV system is represented by

$$\mathbf{M}(t)\ddot{\mathbf{x}}(\mathbf{t}) + \mathbf{D}(t)\dot{\mathbf{x}}(t) + \mathbf{K}(t)\mathbf{x}(t) = \mathbf{bu}(t), \tag{1}$$

where $\mathbf{M}(t)$, $\mathbf{D}(t)$ and $\mathbf{K}(t) \in \Re^{n \times n}$ are mass, damping and stiffness matrices that are functions of time, respectively, $\mathbf{x}(t) \in \Re^n$ is the displacement vector, $\mathbf{b} \in \Re^{n \times n_i}$ is the input shape matrix and $\mathbf{u}(t) \in \Re^{n_i}$ is the input force vector, respectively. The notation $\Re^i$ denotes the i-dimensional real vector space and $\Re^{i \times i}$ denotes the $i \times i$ real matrix space. The following assumptions are used in this study. The elements of the mass, damping and stiffness matrices are bounded and have a finite number of the first order discontinuous points within the interval of interest. The system is asymptotically stable. The mass, damping and stiffness matrices are non-singular and symmetric within the interval of interest. The degree-of-freedom of the system is constant or the system does not degenerate during the period of interest. A state-space model for the system of equation (1) is given by

$$\dot{\mathbf{y}}(t) = \mathbf{A}(t)\mathbf{y}(t) + \mathbf{B}(t)\mathbf{u}(t), \; \mathbf{z}(t) = \mathbf{C}\mathbf{y}(t), \tag{2}$$

where

$$\mathbf{A}(t) = \begin{bmatrix} -\mathbf{M}^{-1}(t)\mathbf{D}(t) & -\mathbf{M}^{-1}(t)\mathbf{K}(t) \\ \mathbf{I} & 0 \end{bmatrix}, \quad \mathbf{B}(t) = \begin{bmatrix} \mathbf{M}^{-1}(t)\mathbf{b} \\ 0 \end{bmatrix}, \quad \mathbf{y}(t) = \begin{bmatrix} \dot{\mathbf{x}}(t) \\ \mathbf{x}(t) \end{bmatrix}.$$

In the above equations, the matrix $\mathbf{A}(t) \in \Re^{2n \times 2n}$ is called the system matrix, $\mathbf{y}(t) \in \Re^{2n}$ is the state variable vector, the matrix $\mathbf{C} \in \Re^{n_o \times 2n}$ is called the output influence matrix, $\mathbf{z}(t) \in \Re^{n_o}$ is the output or response vector and $\mathbf{I} \in \Re^{n \times n}$ is a unit matrix. In the most general case, the matrix $\mathbf{C}$ may be time-dependent as well. In this study, the matrix $\mathbf{C}$ is assumed to be a constant matrix, i.e., the measurement system does not vary with time. It is assumed that the system defined by equation (2) is observable. If the output data are measured at discrete times with a sampling interval τ and the input is a discrete signal characterized by a zero-order hold between consecutive sample points, the corresponding discrete-time state-space representation is of the form

$$\mathbf{y}(k+1) = \mathbf{G}(k)\mathbf{y}(k) + \mathbf{H}(k)\mathbf{u}(k), \; \mathbf{z}(k) = \mathbf{C}\mathbf{y}(k), \tag{3}$$

where $\mathbf{G}(k) \in \Re^{2n \times 2n}$ and $\mathbf{H}(k) \in \Re^{2n \times n_i}$ are not constant and in general their closed forms are unknown. The matrix $\mathbf{G}(k)$ is called the discrete-time state transition matrix. The solution to equation (3) is given by

$$\mathbf{z}(k) = \mathbf{C}\mathbf{G}(k, k_0)\mathbf{y}(k_0) + \mathbf{C}\sum_{j=k_0}^{k-1} \mathbf{G}(k, j+1)\mathbf{H}(j)\mathbf{u}(j), \quad k > k_0 \geqslant 0, \tag{4}$$

where $\mathbf{G}(k, k_0)$ is the state transition matrix from the state at moment k_0 to the state at moment k and is defined as

$$\mathbf{G}(k, k_0) = \begin{cases} \mathbf{G}(k-1)\mathbf{G}(k-2) \ldots \mathbf{G}(k_0), & k > k_0, \\ \mathbf{I}, & k = k_0, \\ \text{undefined}, & k < k_0. \end{cases} \tag{5}$$

It is noted that $\mathbf{G}(k+1, k) = \mathbf{G}(k)$.

2.1. MODAL PARAMETERS OF LTI SYSTEMS

If the system is time-invariant, i.e., **A** and **B** are constant, the discrete-time state transition matrix is a constant matrix given by

$$\mathbf{G}(k) = \mathbf{G} = \exp(\mathbf{A}\tau). \tag{6}$$

In this case, the modal parameters of the system are related to the eigenvalues of **G**. Conducting an eigendecomposition on **G** results in

$$\mathbf{G} = \mathbf{V}\Lambda\mathbf{V}^{-1}, \tag{7}$$

where **V** is the eigenvector matrix and Λ is the diagonal eigenvalue matrix, i.e.,

$$\Lambda = \mathrm{diag}(\lambda_1\ \lambda_2,\ \ldots,\ \lambda_{2n}) \tag{8}$$

with the ith eigenvalue $\lambda_i = \exp(-\delta_i\tau + \mathrm{j}\omega_{di}\tau)$, in which δ_i is the ith damping rate, ω_{di} is the ith damped natural frequency, and $\mathrm{j} = \sqrt{-1}$. As long as **M**, **C** and **K** are real, symmetric, positive definite, and the system is underdamped, the $2n$ eigenvalues occur in complex conjugate pairs, i.e., $\lambda_i = \lambda^*_{i+n}$, $i = 1, 2, \ldots, n$. The similarity transformation is an important feature in a state-space model of LTI systems. If $\mathbf{T} \in \Re^{2n\times 2n}$ is a non-singular matrix, then

$$\bar{\mathbf{G}} = \mathbf{T}\mathbf{G}\mathbf{T}^{-1} \tag{9}$$

is said to be similarly equivalent to **G**. It is easy to see that **G** and $\bar{\mathbf{G}}$ have the same eigenvalues.

2.2. PSEUDO-MODAL PARAMETERS OF LTV SYSTEMS

In a previous work [9], the concept of instantaneous pseudo-modal parameters was introduced using eigenvalues of $\mathbf{G}(k)$ by analogy to LTI systems. The following discussion further explores the use of the pseudo-modal parameters to characterize the dynamic properties of LTV systems. As assumed previously, the system concerned in this study is observable. Therefore, the state transition matrix $\mathbf{G}(k)$ is non-singular at any moment k [17] and the eigensolution of $\mathbf{G}(k)$ exists, i.e.,

$$\mathbf{G}(k) = \mathbf{V}(k)\Lambda(k)\mathbf{V}^{-1}(k), \tag{10}$$

where $\mathbf{V}(k)$ and $\Lambda(k)$ are the eigenvector matrix and eigenvalue matrix, respectively. Because the elements of $\mathbf{G}(k)$ are real, the complex eigenvalues of $\mathbf{G}(k)$ occur in complex conjugate pairs. If the ith eigenvalue $\lambda_i(k)$ is complex, then the following expression can be employed:

$$\lambda_i(k) = \lambda^*_{i+n}(k) = \exp[-\delta_i(k)\tau + \mathrm{j}\omega_{di}(k)\tau], \tag{11}$$

where $-\delta_i(k)$ and $\omega_{di}(k)$ are referred to as the ith pseudo-damping rate and pseudo-damped natural frequency respectively. It is likely that some or all of the

eigenvalues of $\mathbf{G}(k)$ may become real due to a variation in the system parameters. If all the eigenvalues are distinct and the ith eigenvalue $\lambda_i(k)$ is real, its corresponding pseudo-damped natural frequency is zero or $\omega_{di}(k) = 0$ and its corresponding pseudo-damping rate equals $-\delta_i(k) = \ln[\lambda_i(k)]/\tau$. Normally, real eigenvalues of $\mathbf{G}(k)$ also occur in pairs. For example, if $\lambda_i(k) = a + b$ is real, $\lambda_{i+n}(k) = a - b$. This implies that if $\lambda_i(k)$ increases, $\lambda_{i+n}(k)$ decreases.

Two special types of LTV systems are abrupt and periodic. The parameters of an abrupt change system vary from an old status $\mathbf{A}^{old}$ when $t < k_0\tau$ to a new status $\mathbf{A}^{new}$ when $k_0\tau \leqslant t$. In this case, the discrete-time state transition matrix is known,

$$\mathbf{G}(k) = \begin{cases} \exp(\mathbf{A}^{old}\tau), & 0 \leqslant k < k_0, \\ \exp(\mathbf{A}^{new}\tau), & k_0 \leqslant k. \end{cases} \tag{12}$$

Therefore, the pseudo-modal parameters are equal to the modal parameters defined by the conventional definition. An abrupt change in the system parameters results in a sudden variation in the modal parameters.

The parameter matrices of a periodic change system with a period T satisfy the relation

$$\mathbf{A}(t + T) = \mathbf{A}(t) \text{ and } \mathbf{B}(t + T) = \mathbf{B}(t). \tag{13}$$

If the period is discretized as $T = P\tau$, according to Floquet theory [4], the discrete-time state transition matrix $\mathbf{G}(k)$ has the form

$$\mathbf{G}(k, k_0) = \mathbf{R}(k, k_0)\exp[\mathbf{F}(k - k_0)\tau],\ \mathbf{G}(k) = \mathbf{G}(k + 1, k) = \mathbf{R}(k)\exp(\mathbf{F}\tau), \tag{14}$$

where $\mathbf{R}(k, k_0) \in \Re^{2n \times 2n}$ is a periodic matrix, i.e., $\mathbf{R}(k + P) = \mathbf{R}(k)$, $\exp(\mathbf{F}\tau) \in \Re^{2n \times 2n}$ and $\mathbf{F}$ is a constant matrix. The pseudo-modal parameters are periodic because the state transition matrix is periodic or $\mathbf{G}(k + P) = \mathbf{G}(k)$.

2.3. STABILITY OF LTV SYSTEMS

As the conventional modal parameters, the pseudo-modal parameters can be used to study the system stability. It has been proven that if a varying system is asymptotically stable, the following condition holds [17]:

$$\mathbf{G}(k, k_0) \to 0 \quad \text{when } k \to \infty. \tag{15}$$

This implies that for any non-zero initial condition, the free response of the asymptotically stable system approaches zero when $k \to \infty$. This condition is satisfied if all the eigenvalues of $\mathbf{G}(k)$, $k > k_0$, lie within the unit circle in the complex plane, i.e., $|\lambda_i(k)| < 1$ or $-\delta_i(k) < 0$ for $i = 1,2, \ldots, 2n$. Therefore, the values of the pseudo-damping rates are an indicator of the instantaneous stability of the system. If some of the eigenvalues of $\mathbf{G}(k)$ are outside of the unit circle temporarily, the system may become temporarily unstable.

For a periodic system, the transition matrix over a period of the parameter variation is a constant matrix and is denoted as $\mathbf{G}(k + P, k)$. Thus, the transition

matrix over m periods is given by

$$\begin{aligned}\mathbf{G}(k+mP,k) &= \mathbf{G}[k+mP,k+(m-1)P]\mathbf{G}[k+(m-1)P,k+(m-2)P]\ldots \\ &\quad \times \mathbf{G}(k+P,k) \\ &= \mathbf{G}^m(k+P,k). \end{aligned} \tag{16}$$

The eigenvalues $\lambda_i(k+P,k)$ of $\mathbf{G}(k+P,k)$, which are called the Floquet multipliers [4], determine the stability of the periodic system. Let $k=0$ and $\mathbf{R}(0,0)=\mathbf{I}$,

$$\mathbf{G}(P,0) = \mathbf{R}(P,0)\exp(\mathbf{F}P\tau) = \mathbf{R}(0,0)\exp(\mathbf{F}P\tau) = \exp(\mathbf{F}P\tau). \tag{17}$$

Therefore, the eigenvalues of $\mathbf{G}(P,0)$ are directly related to the eigenvalues of $\mathbf{F}$. If any of the eigenvalues of $\mathbf{F}$ lie in the right-half complex plane, the periodic system is unstable. Since $\mathbf{G}(k)=\mathbf{R}(k)\exp(\mathbf{F}\tau)$, the eigenvalues of $\mathbf{G}(k)$ are affected by the eigenvalues of $\mathbf{F}$.

2.4. VARYING MODAL PARAMETERS

In some references [5–8], so-called varying modal parameters are evaluated using the conventional definition by treating the matrix $\mathbf{A}(t)$ as a constant matrix at the moment of consideration. The varying modal parameters can be considered as an approximation of the pseudo-modal parameters as shown below. An approximate form of a general discrete-time state transition matrix can be obtained using the series expansions

$$\begin{aligned}\mathbf{G}(k) = \mathbf{I} &+ \mathbf{A}(k)\tau + \frac{1}{2}[\mathbf{A}^2(k) + \dot{\mathbf{A}}(k)]\tau^2 \\ &+ \frac{1}{3!}[\mathbf{A}^3(k) + \mathbf{A}(k)\dot{\mathbf{A}}(k) + 2\dot{\mathbf{A}}(k) + \ddot{\mathbf{A}}(k)]\tau^3 + \cdots. \end{aligned} \tag{18}$$

The above equation indicates that the changes in the pseudo-modal parameters depend on the variability of the system matrix $\mathbf{A}(k)$. If the derivatives, $\dot{\mathbf{A}}(k)$, $\ddot{\mathbf{A}}(k)$, … , are small or the system is slowly varying, the discrete-time state transition matrix $\mathbf{G}(k)$ can be approximated by

$$\mathbf{G}(k) \approx \mathbf{I} + \mathbf{A}(k)\tau + \frac{1}{2}\mathbf{A}^2(k)\tau^2 + \frac{1}{3!}\mathbf{A}^3(k)\tau^3 + \cdots = \exp[\mathbf{A}(k)\tau]. \tag{19}$$

This relation can also be derived using the frozen technique [2,18].

2.5. THE SIMILARITY TRANSFORMATION

For time-varying systems, the similarity transformation is defined as

$$\bar{\mathbf{G}}(k) = \mathbf{T}(k+1)\mathbf{G}(k)\mathbf{T}^{-1}(k), \qquad \bar{\mathbf{H}}(k) = \mathbf{T}(k)\mathbf{H}(k), \qquad \bar{\mathbf{C}}(k) = \mathbf{C}\mathbf{T}^{-1}(k), \tag{20}$$

where $\mathbf{T}(k) \in \Re^{2n \times 2n}$ and $\mathbf{T}(k+1) \in \Re^{2n \times 2n}$ are non-singular. The matrices $\bar{\mathbf{G}}(k)$, $\bar{\mathbf{H}}(k)$, and $\bar{\mathbf{C}}(k)$ are another realization of the system. For LTV systems, the similarity transformation preserves the boundedness and stability of the system. However, in general, $\mathbf{G}(k)$ and $\tilde{\mathbf{G}}(k)$ no longer share the same eigenvalues if $\mathbf{T}(k)$ is not equal to $\mathbf{T}(k+1)$. In the following section, the discussion is focused on developing an algorithm to identify the matrix defined as

$$\tilde{\mathbf{G}}(k) = \mathbf{T}(k)\mathbf{G}(k)\mathbf{T}^{-1}(k). \tag{21}$$

The eigenvalues of $\tilde{\mathbf{G}}(k)$ remain same as those of $\mathbf{G}(k)$ as long as $T(k)$ is non-singular.

3. IDENTIFICATION OF THE PSEUDO-MODAL PARAMETERS

This section extends the algorithm developed in reference [9] to the case of using an ensemble of forced responses and inputs. To obtain an ensemble of input–output sequences, N experiments are conducted on the system. In each experiment, the system undergoes the same time-varying change and is excited by a different input. The measurements from the jth experiment are represented by $\mathbf{z}_j(k)$ and $\mathbf{u}_j(k)$, $j \in [1, N]$. Using these N sets of the input and output data from the time instant k to $k + M - 1$, a general output Hankel matrix $\mathbf{Z}(k) \in \Re^{n_o M \times N}$ is formed as

$$\mathbf{Z}(k) = \begin{bmatrix} \mathbf{z}_1(k) & \mathbf{z}_2(k) & \cdots & \mathbf{z}_N(k) \\ \mathbf{z}_1(k+1) & \mathbf{z}_2(k+1) & \cdots & \mathbf{z}_N(k+1) \\ \vdots & \vdots & \ddots & \vdots \\ \mathbf{z}_1(k+M-1) & \mathbf{z}_2(k+M-1) & \cdots & \mathbf{z}_N(k+M-1) \end{bmatrix} \tag{22}$$

and a general input Hankel matrix $\mathbf{U}(k) \in \Re^{n_i M \times \mathrm{N}}$ is formed in the way similar to $\mathbf{Z}(k)$ using $\mathbf{u}_j(k)$, $j \in [1, N]$. In the absence of noise, $\mathbf{Z}(k)$ and $\mathbf{U}(k)$ are related by an input–output matrix equation:

$$\mathbf{Z}(k) = \mathbf{\Gamma}(k)\mathbf{Y}(k) + \Theta(k)\mathbf{U}(k), \tag{23}$$

where the state matrix $\mathbf{Y}(k) \in \Re^{2n \times N}$ is given by

$$\mathbf{Y}(k) = [\mathbf{y}_1(k) \;\; \mathbf{y}_2(k) \;\; \mathbf{y}_3(k) \;\; \cdots \;\; \mathbf{y}_N(k)]. \tag{24}$$

The observability matrix $\mathbf{\Gamma}(k) \in \Re^{n_o M \times 2n}$ is given by

$$\mathbf{\Gamma}(k) = \begin{bmatrix} \mathbf{C} \\ \mathbf{C}\mathbf{G}(k+1, k) \\ \mathbf{C}\mathbf{G}(k+2, k) \\ \vdots \\ \mathbf{C}\mathbf{G}(k+M-1, k) \end{bmatrix}, \tag{25}$$

the impulse response matrix $\Theta(k) \in \Re^{n_o M \times n_i}$ is given by

$$\Theta(k) = [\Theta_1(k)\Theta_2(k), \ldots, \Theta_M(k)], \tag{26}$$

and its ith block matrix in the jth column is of the form

$$\Theta_{ij}(k) = \begin{cases} 0, & i \leqslant j, \\ \mathbf{CH}(k+j-1), & i = j+1, \\ \mathbf{CG}(k+j+i-3, k+j)\mathbf{H}(k+j-1), & i > j+1. \end{cases} \tag{27}$$

An important step of the algorithm proposed in reference [9] is to extract the range space of the observability matrix $\mathbf{\Gamma}(k)$. Let Range ($\mathbf{S}$) denote the range space of a matrix $\mathbf{S}$. If a matrix $\bar{\mathbf{\Gamma}}(k)$ has the same range space as Range($\mathbf{\Gamma}(k)$), such a matrix $\bar{\mathbf{\Gamma}}(k)$ can be written as $\bar{\mathbf{\Gamma}}(k) = \mathbf{\Gamma}(k)\mathbf{T}^{-1}(k)$ for some non-singular matrix $\mathbf{T}(k) \in \Re^{2n \times 2n}$. In order to extract the observability range space, the part of the output $\mathbf{Z}(k)$ that does not emanate from the state $\mathbf{Y}(k)$ needs to be eliminated. In other words, the second term on the right-hand side of equation (23) has to be annihilated. To do this, a matrix $\mathbf{U}^{\perp}(k) \in \Re^{N \times N}$ is needed such that $\mathbf{U}^{\perp}(k)$ is normal to $\mathbf{U}(k)$ or $\mathbf{U}(k)\mathbf{U}^{\perp}(k) = 0$. A simple formulation of $\mathbf{U}^{\perp}(k)$ is given by

$$\mathbf{U}^{\perp}(k) = \mathbf{I} - \mathbf{U}^{\mathrm{T}}(k)[\mathbf{U}(k)\mathbf{U}^{\mathrm{T}}(k)]^{-1}\mathbf{U}(k), \tag{28}$$

where $\mathbf{I} \in \Re^{N \times N}$ is a unit matrix. The indicated inverse exists if the matrix $\mathbf{U}(k)$ has a full row rank, i.e., $\mathrm{rank}(\mathbf{U}(k)) = n_i M \leqslant N$. Postmultiplying equation (23) by $\mathbf{U}^{\perp}(k)$ results in

$$\mathbf{Z}(k)\mathbf{U}^{\perp}(k) = \mathbf{\Gamma}(k)\mathbf{Y}(k)\mathbf{U}^{\perp}(k). \tag{29}$$

Now the range space of the observability matrix can be obtained from $\mathbf{Z}(k)\mathbf{U}^{\perp}(k)$, i.e.,

$$\bar{\mathbf{\Gamma}}(k) = \mathrm{Range}(\mathbf{Z}(k)\mathbf{U}^{\perp}(k)) = \mathrm{Range}(\mathbf{\Gamma}(k))$$

$$= \begin{bmatrix} \bar{\mathbf{C}}(k) \\ \bar{\mathbf{C}}(k+1)\bar{\mathbf{G}}(k) \\ \bar{\mathbf{C}}(k+2)\bar{\mathbf{G}}(k+1)\bar{\mathbf{G}}(k) \\ \vdots \\ \bar{\mathbf{C}}(k+M-1)\bar{\mathbf{G}}(k+M-1, k) \end{bmatrix}. \tag{30}$$

To extract $\bar{\mathbf{\Gamma}}(k+1)$, $\mathbf{Z}(k+1)$ and $\mathbf{U}(k+1)$ are formed using the data from the moment $k+1$ to the moment $k+M$ and they satisfy the relation

$$\mathbf{Z}(k+1) = \mathbf{\Gamma}(k+1)\mathbf{Y}(k+1) + \mathbf{\Theta}(k+1)\mathbf{U}(k+1). \tag{31}$$

Then one has

$$\bar{\mathbf{\Gamma}}(k+1) = \text{Range}(\mathbf{Z}(k+1)\mathbf{U}^{\perp}(k+1)) = \text{Range}(\mathbf{\Gamma}(k+1))$$

$$= \begin{bmatrix} \bar{\mathbf{C}}(k+1) \\ \bar{\mathbf{C}}(k+2)\bar{\mathbf{G}}(k+1) \\ \bar{\mathbf{C}}(k+3)\bar{\mathbf{G}}(k+2)\bar{\mathbf{G}}(k+1) \\ \vdots \\ \bar{\mathbf{C}}(k+M)\bar{\mathbf{G}}(k+M, k+1) \end{bmatrix}. \tag{32}$$

Two matrices $\bar{\mathbf{\Gamma}}_1(k+1)$ and $\bar{\mathbf{\Gamma}}_2(k)$ are formed using the first $M-1$ block rows of $\bar{\mathbf{\Gamma}}(k+1)$ and the last $M-1$ block rows of $\bar{\mathbf{\Gamma}}(k)$ respectively:

$$\bar{\mathbf{\Gamma}}_1(k+1) = \begin{bmatrix} \bar{\mathbf{C}}(k+1) \\ \bar{\mathbf{C}}(k+2)\bar{\mathbf{G}}(k+1) \\ \bar{\mathbf{C}}(k+3)\bar{\mathbf{G}}(k+2)\bar{\mathbf{G}}(k+1) \\ \vdots \\ \bar{\mathbf{C}}(k+M-1)\bar{\mathbf{G}}(k+M-1, k+1) \end{bmatrix} \tag{33}$$

and

$$\bar{\mathbf{\Gamma}}_2(k) = \begin{bmatrix} \bar{\mathbf{C}}(k+1)\bar{\mathbf{G}}(k) \\ \bar{\mathbf{C}}(k+2)\bar{\mathbf{G}}(k+1)\bar{\mathbf{G}}(k) \\ \bar{\mathbf{C}}(k+3)\bar{\mathbf{G}}(k+2)\bar{\mathbf{G}}(k+1)\bar{\mathbf{G}}(k) \\ \vdots \\ \bar{\mathbf{C}}(k+M-1)\bar{\mathbf{G}}(k+M-1, k) \end{bmatrix}. \tag{34}$$

Now an estimate for $\bar{\mathbf{G}}(k)$ can be found by

$$\bar{\mathbf{G}}(k) = [\bar{\mathbf{\Gamma}}_1(k+1)]^{+}\bar{\mathbf{\Gamma}}_2(k), \tag{35}$$

where $(\mathbf{S})^{+}$ denotes the Moore–Penrose inverse of a matrix $\mathbf{S}$.

To extract the range space $\bar{\mathbf{\Gamma}}(k)$ or $\bar{\mathbf{\Gamma}}(k+1)$, the singular-value decomposition (SVD) [19] can be employed:

$$\mathbf{Z}(k)\mathbf{U}^{\perp}(k) = \mathbf{\Phi}(k)\mathbf{\Sigma}(k)\mathbf{\Psi}^{\mathrm{T}}(k),$$

$$\mathbf{Z}(k+1)\mathbf{U}^{\perp}(k+1) = \mathbf{\Phi}(k+1)\mathbf{\Sigma}(k+1)\mathbf{\Psi}^{\mathrm{T}}(k+1). \tag{36}$$

According to the property of the SVD, the first $2n$ columns of $\mathbf{\Phi}(k)$ give a set of the base vectors for the range space of $\mathbf{\Gamma}(k)$, i.e.,

$$\bar{\mathbf{\Gamma}}(k) = \mathbf{\Phi}_s(k) = [\mathbf{\Phi}_1(k), \mathbf{\Phi}_2(k), \ldots, \mathbf{\Phi}_{2n}(k)] \tag{37}$$

and the same holds for the first $2n$ columns of $\mathbf{\Phi}(k+1)$, i.e.,

$$\bar{\mathbf{\Gamma}}(k+1) = \mathbf{\Phi}_s(k+1) = [\mathbf{\Phi}_1(k+1), \mathbf{\Phi}_2(k+1), \ldots, \mathbf{\Phi}_{2n}(k+1)]. \tag{38}$$

Now invoking equations (33)–(35) results in $\tilde{\mathbf{G}}(k)$.

In order to find $\tilde{\mathbf{G}}(k)$, the matrix $\mathbf{T}(k)\mathbf{T}^{-1}(k+1)$ is needed. However, the exact form of $\mathbf{T}(k)\mathbf{T}^{-1}(k+1)$ is unknown. In a special case when $n_o \geqslant 2n$ and the rank of $\mathbf{C}$ is equal to $2n$, the matrix $\mathbf{T}(k)\mathbf{T}^{-1}(k+1)$ can be obtained by

$$\mathbf{T}(k)\mathbf{T}^{-1}(k+1) = \mathbf{F}^{+}(k)\mathbf{F}(k+1), \tag{39}$$

where $\mathbf{F}(k)$ and $\mathbf{F}(k+1)$ are formed by the first n_o rows of $\mathbf{\Phi}_s(k)$ and $\mathbf{\Phi}_s(k+1)$ respectively. If $n_o < 2n$, an approximate form of $\mathbf{T}(k)\mathbf{T}^{-1}(k+1)$ can be obtained using the method suggested in reference [9]. Finally, the matrix $\tilde{\mathbf{G}}(k)$ is given by

$$\tilde{\mathbf{G}}(k) = \mathbf{F}^{+}(k)\mathbf{F}(k+1)\{[\bar{\mathbf{\Gamma}}_1(k+1)]^{+}\bar{\mathbf{\Gamma}}_2(k)\}. \tag{40}$$

The algorithm described above is summarized as follows: To find $\tilde{\mathbf{G}}(k_0+i)$, $i = 0, 1, 2, \ldots, l$, (1) construct the general Hankel matrices, $\mathbf{Z}(k_0+i)$ and $U(k_0+i)$. Find the matrix $\mathbf{U}^{\perp}(k_0+i)$ using equation (28). (2) Conduct the SVD on $\mathbf{Z}(k_0+i)\mathbf{U}^{\perp}(k_0+i)$ to obtain $\mathbf{\Phi}_s(k_0+i)$. (3) Construct the general Hankel matrices $\mathbf{Z}(k_0+i+1)$ and $\mathbf{U}(k_0+i+1)$. Find the matrix $\mathbf{U}^{\perp}(k_0+i+1)$ using equation (28). (4) Conduct the SVD on $\mathbf{Z}(k_0+i+1)\mathbf{U}^{\perp}(k_0+i+1)$ to obtain $\mathbf{\Phi}_s(k_0+i+1)$. (5) Use $\mathbf{\Phi}_s(k_0+i)$ and $\mathbf{\Phi}_s(k_0+i+1)$ to form $\bar{\mathbf{\Gamma}}_2(k_0+i)$, $\bar{\mathbf{\Gamma}}_1(k_0+i+1)$, $\mathbf{F}(k_0+i)$, and $\mathbf{F}(k_0+i+1)$, (6) Solve equation (40) to obtain $\tilde{\mathbf{G}}(k_0+i)$. If $i < l$, increase i by 1 and go to Step 3.

4. AN ILLUSTRATIVE EXAMPLE

The purpose of the example given in this section is two-fold. First, it serves to illustrate how the pseudo-modal parameters can be used to characterize the dynamics of LTV systems. Second, it tests the proposed algorithm under different conditions. A planar robotic manipulator with varying inertia links is used as a LTV system and shown in Figure 1. The manipulator is placed in a horizontal plan and each link has a sliding mass μ_i whose position $r_i(t)$ can be varied. Such a manipulator was discussed in reference [20] and the idea of the use of time-varying inertia links is to compensate external perturbation by varying the position of the sliding masses. To model the system, the following assumptions are used. The links are uniform rigid bars of equal length l and mass m. The first link is connected to the base by means of an elastic spring-hinge of rotational stiffness k_1. The second link is connected to the first link by a similar spring of stiffness k_2. The viscous damping is modelled by the rotary dampers d_1 and d_2. The angles φ_1 and φ_2 denote the angular positions of the links relative to the x-axis. When disturbed, the links vibrate about their equilibrium positions φ_{10} and φ_{20}. The actual angular positions of the links become $\varphi_1 = \varphi_{10} + \varphi_{11}$ and $\varphi_2 = \varphi_{20} + \varphi_{21}$. With the assumption of small angular vibrations, a linearized model for the system is defined by a matrix equation

$$\mathbf{M}(t)\ddot{\varphi} + \mathbf{D}(t)\dot{\varphi} + \mathbf{K}\varphi = \mathbf{q}(t), \tag{41}$$

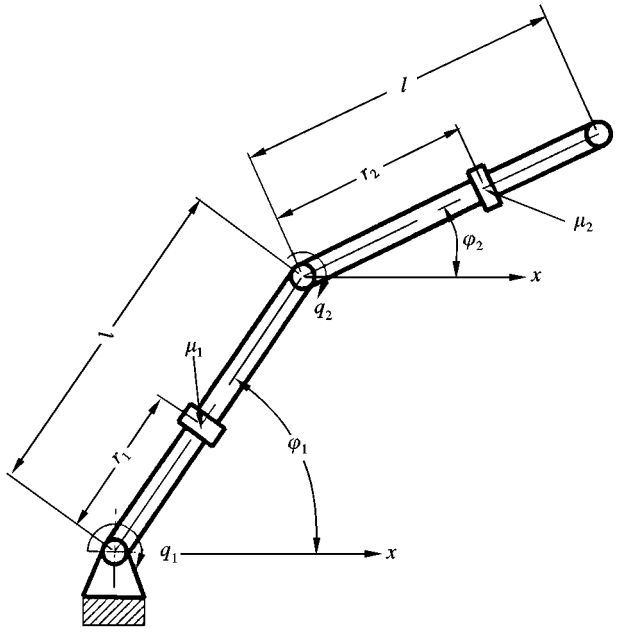

Figure 1. A robotic manipulator with varying inertia links.

where $\varphi = [\varphi_{11}\varphi_{21}]^{\mathrm{T}}$, and where

$$\mathbf{M}(t) = \begin{bmatrix} a_1 + \mu_2 l^2 + \mu_1 r_1^2 & (a_2 + \mu_2 l r_2)\cos(\Delta\varphi_0) \\ (a_2 + \mu_2 l r_2)\cos(\Delta\varphi_0) & a_3 + \mu_2 r_2^2 \end{bmatrix},$$

$$\mathbf{D}(t) = \begin{bmatrix} d_1 + d_2 + 2\mu_1 r_1 \dot{r}_1 & -d_2 + \mu_2 l \dot{r}_2 \cos(\Delta\varphi_0) \\ -d_2 + \mu_2 l \dot{r}_2 \cos(\Delta\varphi_0) & d_2 + 2\mu_2 r_2 \dot{r}_2 \end{bmatrix},$$

$$\mathbf{K} = \begin{bmatrix} k_1 + k_2 & -k_2 \\ -k_2 & k_2 \end{bmatrix}, \qquad \mathbf{q}(t) = \begin{bmatrix} q_1(t) - q_2(t) \\ q_2(t) \end{bmatrix},$$

$$a_1 = 4ml^2/3,\ a_2 = ml^2/2,\ a_3 = ml^2/3,\ \Delta\varphi_0 = \varphi_{10} - \varphi_{20}.$$

The state vector is defined as $\mathbf{y} = [\dot{\varphi}^{\mathrm{T}}, \varphi^{\mathrm{T}}]^{\mathrm{T}}$.

In the simulation, the following numerical quantities were used: the length $l = 1$ m, the mass $m = 2$ kg, the sliding masses $\mu_1 = \mu_2 = 0{\cdot}5$ kg, the stiffness $k_1 = 100$ N m/rad, $k_2 = 80$ N m/rad, and the damping coefficients $d_1 = 0{\cdot}5$ N m/rad/s, $d_2 = 0{\cdot}4$ N m/rad/s. Because a closed-form of the time-varying transition matrix of the system under study is unknown, the true transition matrices were found using a numerical way given in reference [9]. After the transition matrix at each instant was found, an eigendecomposition was conducted on the true transition matrix to obtain the varying eigenvalues and the pseudo-modal parameters defined by equation (11).

4.1. THE PSEUDO-MODAL PARAMETERS AND VARYING PATTERNS OF SLIDING MASSES

In the use of the sliding masses as a means of vibration control, it is desirable to have a good understanding of the dynamic behaviors of the robot under different varying patterns of the sliding masses. A straightforward way would be to study changes in individual elements of the mass and damping matrices for various varying patterns. However, such information is indirectly related to the dynamics of the robot. On the other hand, the discrete-timestate transition matrices and the pseudo-modal parameters provide some global characteristics of the robot. To illustrate this idea, the following simulation scenario is used. Initially, the sliding masses remain at r_1^{old} and r_2^{old} in the period of $0 \leqslant t \leqslant 1$ s. Then, during the period of $1 \leqslant t \leqslant 4$ s, the sliding masses change their positions in a given pattern. Finally, the positions of the sliding masses become r_1^{new} and r_2^{new}. The configuration of the manipulator is $\Delta\varphi_0 = 45^\circ$. Four cases of changes in the initial and final positions are considered:

$$\begin{aligned}
&\textit{Case 1:}\ r_1^{old} = r_2^{old} = 0{\cdot}1,\ r_1^{new} = r_2^{new} = 0{\cdot}9;\\
&\textit{Case 2:}\ r_1^{old} = 0{\cdot}9,\ r_2^{old} = 0{\cdot}1,\ r_1^{new} = 0{\cdot}1,\ r_2^{new} = 0{\cdot}9;\\
&\textit{Case 3:}\ r_1^{old} = r_2^{old} = 0{\cdot}9,\ r_1^{new} = r_2^{new} = 0{\cdot}1;\\
&\textit{Case 4:}\ r_1^{old} = 0{\cdot}1,\ r_2^{old} = 0{\cdot}9,\ r_1^{new} = 0{\cdot}9,\ r_2^{new} = 0{\cdot}1.
\end{aligned}$$

First let the movement of the sliding masses have a trapezoidal velocity profile, i.e.,

$$\dot{r}_i(t) = \begin{cases} \dot{r}_{ic}(t-1), & 1 \leqslant t \leqslant 2,\\ \dot{r}_{ic}, & 2 < t \leqslant 3,\\ \dot{r}_{ic}(4-t), & 3 < t \leqslant 4, \end{cases} \tag{42}$$

where $i = 1, 2$ and $\dot{r}_{ic} = (r_i^{new} - r_i^{odd})/2$ is the maximum constant velocity. In the following simulation, a sampling interval $\tau = 0{\cdot}04$ s was used. The pseudo-damped natural frequencies $\omega_{d1}(k)$ and $\omega_{d2}(k)$ for all four cases are given in Figures 2(a) and (b), respectively. The pseudo damping rates $-\delta_1(k)$ and $-\delta_2(k)$ for all four cases are given in Figures 3(a) and (b), respectively. Several observations can be drawn from the figures. In general, the variation of the pseudo-modal parameters consists of three phases, that is, the old constant values, the varying values and the new constant values. The changes from the constant values to the varying values are continuous. The continuity of the values is determined by the nature of the parameters in the mass and damping matrices and the trapezoidal velocity profile. With such a variation pattern, at moments $t = 1$ and 4 s, the changes in the positions and velocities of the sliding masses are continuous and the changes in the acceleration are abrupt. Because the mass and damping matrices are functions of r_i and $\dot{r}_i$, the transition in the pseudo-modal parameters is continuous. It is noted that, in Cases 3 and 4, $-\delta_1(k)$ becomes positive in a portion of the varying period. Such a behavior is explained by the changes in the damping matrix $\mathbf{D}(t)$. Because of changes in $\dot{r}_1(t)$ and $\dot{r}_2(t)$, the effective system damping is reduced.

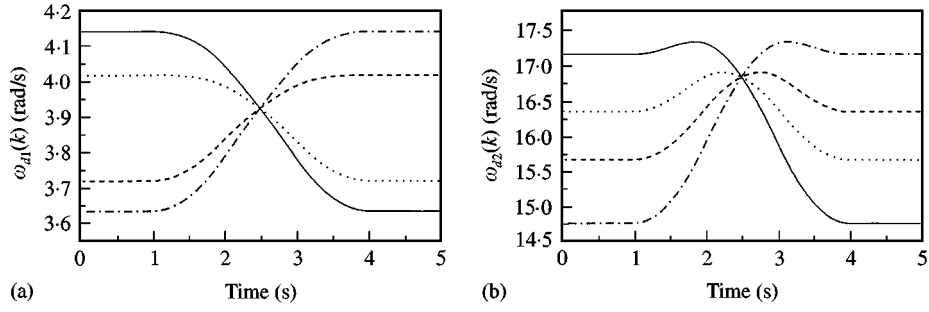

Figure 2. Pseudo-damped natural frequencies for a variation of the trapezoidal velocity profile: ——, case 1; ……, case 2; _·_·_·_, case 3; – – – –, case 4. (a) $\omega_{d1}(k)$; (b) $\omega_{d2}(k)$.

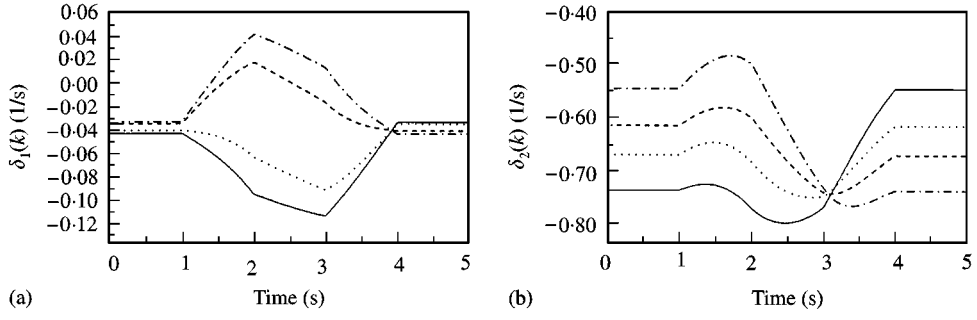

Figure 3. Pseudo-damping rates for a variation of the trapezoidal velocity profile: ——, case 1; ……, case 2; _·_·_·_, case 3; – – – –, case 4. (a) $-\delta_{d1}(k)$; (b) $-\delta_{d2}(k)$.

Now let the sliding masses move with a sinusoidal position profile, i.e.,

$$r_i(t) = r_i^{old} + (r_i^{new} - r_i^{old}) \sin[\pi(t-1)/6], \quad 1 \leqslant t \leqslant 4 \text{ s}. \tag{43}$$

The pseudo-damped natural frequencies for all four cases are shown in Figures 4(a) and (b), while the pseudo-damping rates for all four cases are given in Figures 5 (a) and (b). It is noted that the changes in the values are not continuous at the beginning of the variation. This is caused by a sudden change in $\dot{r}_i(t)$, which results is an abrupt variation in the effective damping matrix. It is also seen that, in Cases 3 and 4, $-\delta_1(k)$ has a larger increase than the value with the trapezoidal velocity profile.

4.2. IDENTIFICATION OF THE PSEUDO-MODAL PARAMETERS

The forced responses are obtained by applying a torque at joint one. The torque applied at joint two is zero. It is assumed that the state variables are directly available, i.e., $\mathbf{C} = \mathbf{I}$ or $\mathbf{z}_j(k) = \mathbf{y}_j(k) = [\dot{\varphi}_{11j}(k)\ \dot{\varphi}_{12j}(k)\ \varphi_{11j}(k)\ \varphi_{12}(k)]^{\mathrm{T}}$. The dimensions of the state-space model are $2n = 4$, $n_i = 1$ and $n_o = 4$.

The statistical quantities that were used in the simulation are defined in the same manner as those in reference [15]. For a discrete stochastic process, for example, v_j,

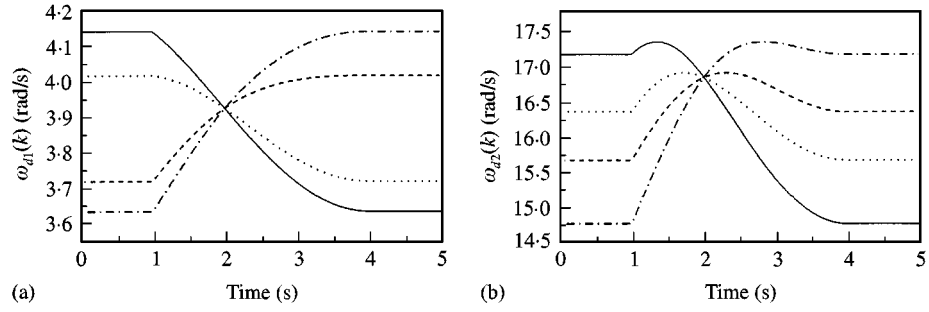

Figure 4. Pseudo-damped natural frequencies for a variation of the sinusoidal position profile: ——, case 1; ……, case 2; –·–·–·–, case 3; – – – –, case 4. (a) $\omega_{d1}(k)$; (b) $\omega_{d2}(k)$.

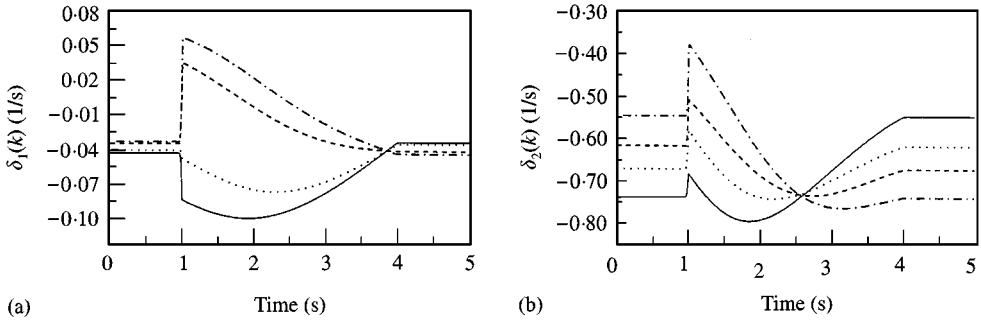

Figure 5. Pseudo damping rates for a variation of the sinusoidal position profile: ——, case 1; ……, case 2; –·–·–·–, case 3; – – – –, case 4. (a) $-\delta_{d1}(k)$; (b) $-\delta_{d2}(k)$.

$v_j(k)$ presents the observation in the jth experiment at moment k. An ensemble of $v_j(k)$ is a family of values $v_j(k)$ for $j \in [1, N]$. For a specific moment k, $v_j(k)$ is a random variable, the mean and standard deviation of $v_j(k)$ are defined as

$$\bar{v}(k) = \frac{1}{N}\sum_{j=1}^{N} v_j(k),\ \sigma_v(k) = \sqrt{\frac{1}{N}\sum_{j=1}^{N}[v_j(k) - \bar{v}(k)]^2}. \tag{44}$$

It is assumed that the responses are contaminated by measurement noise. The signal-to-noise ratio (SNR) is defined as

$$SNR = \sigma_{z_i}(k)/\sigma_{w_i}(k), \quad i = 1, 2, 3, 4, \tag{45}$$

where $\sigma_{z_i}(k)$ is the standard deviation of the ith response at moment k and $\sigma_{w_i}(k)$ is the standard deviation of the noise added to the ith output at moment k. In the simulation, the output sequences $\mathbf{z}_j(k), j \in [1, N]$, were numerically found using the Runge–Kutta integrator. Then $\sigma_{z_i}(k)$ was found using the ith output $z_{ij}(k)$, $j \in [1, N]$, in equation (44). With a given SNR, $\sigma_{w_i}(k)$ was determined by equation (45). Finally, a Gaussian white noise series with a unit standard deviation was multiplied by the value $\sigma_{w_i}(k)$ to generate a series $\mathbf{w}_i(k) = [w_{i1}(k), w_{12}(k), \ldots, w_{iN}(k)]$. The noisy output $\hat{z}_{ij}(k)$ was obtained as $\hat{z}_{ij}(k) = z_{ij}(k) + w_{ij}(k)$.

It is important to select M or N properly. The block row number M should be chosen such that $n_o M > 2n$. A larger M implies that the extracted subspace is valid over a longer time interval. In this sense, a larger M is better. On the other hand, M determines the row number $n_i M$ of $\mathbf{U}(k)$ which should be less than the column number N, i.e., $n_i M < N$ to ensure the existence of $[\mathbf{U}(k)\mathbf{U}^T(k)]^{-1}$ in equation (28). Therefore, an increase of M will cause an increase of N and result in a drastic increase of testing and computational cost. In the following simulation, $N = 20$ and $M = 5$ were used if it is not stated otherwise.

It is very critical to ensure that the input is persistently exciting. The success of the algorithm depends very much on the quality of the inversion of $\mathbf{U}(k)\mathbf{U}^{\mathrm{T}}(k)$. The input sequences are persistently exciting at the time-instant k if the rank of $\mathbf{U}(k)$ equals $n_i M$. To ensure this condition, there must be at least $n_i M$ sets of independent inputs among N sets of input sequences. A white noise input is a persistent excitation. Therefore, as long as N sets of white noise series are generated independently, the rank of $\mathbf{U}(k)$ equals $n_i M$.

Figures 6(a) and (b) show a comparison of the true values and the estimated values for $\omega_{d1}(k)$ and $-\delta_1(k)$ respectively. The sliding masses were engaged in the movement of Case B with the trapezoidal velocity profile. The sliding masses start moving at $t = 3$ s to give a sufficient time to excite the system. The signal-to-noise ratio was 50. The figures give the values of a single estimate and mean values of 10 estimates. Figures 7(a) and (b) show the results when SNR = 100 was used. For each experiment, a white noise with a unit variance was generated as the input $q_1(k)$ and the initial states of the system were zero. The figures show that the estimated pseudo-parameters follow the variation of the true values. When the noise level is lower or SNR is larger, the accuracy of estimation improves. The estimated pseudo-damping rates are more sensitive to the noise disturbance than the estimated pseudo-damped natural frequencies. The results of a single estimate are not satisfactory and more estimates will improve the results.

To measure the quality of estimates, the standard deviation of estimated values is used. For example, the standard deviation of $\omega_{d1}(k)$ is defined as

$$\sigma_{\omega_{d1}(k)} = \sqrt{\frac{1}{L}\sum_{i=1}^{L}[\omega_{d1l}(k) - \bar{\omega}_{d1}(k)]^2}, \tag{46}$$

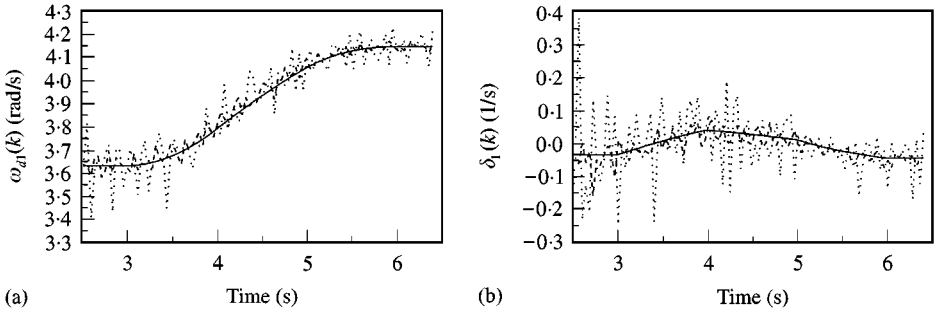

Figure 6. Comparison of the true and estimated values of the first pseudo-damped natural frequency and pseudo-damping rate when SNR = 50: ——, true values; ……, values of a single estimate; – – – –, mean values of 10 estimates. (a) $\omega_{d1}(k)$; (b) $-\delta_{d1}(k)$.

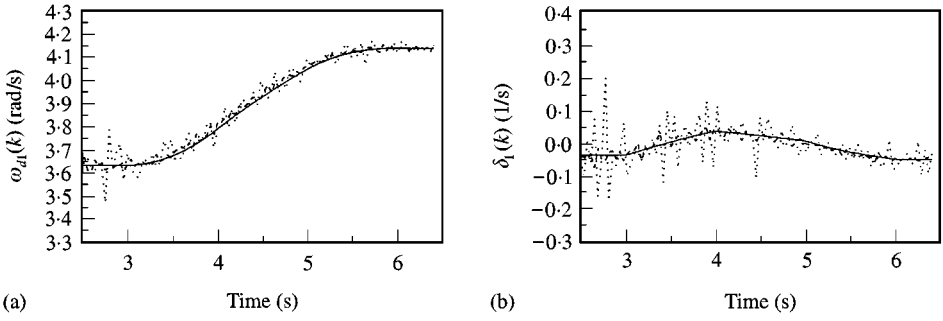

Figure 7. Comparison of the true and estimated values of the first pseudo-damped natural frequency and pseudo-damping rate when SNR = 100: ——, true values; ……, values of a single estimate; – – – –, mean values of 10 estimates. (a) $\omega_{d1}(k)$; (*b*) – $\delta_{d1}(k)$.

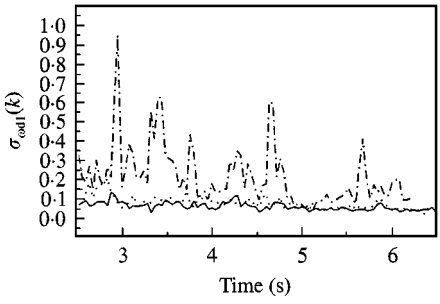

Figure 8. Standard deviation values $\sigma_{\omega_{d1}(k)}$ of the estimated pseudo-damped natural frequencies: ——, $M = 5$; ……, $M = 10$; _·_·_·_, $M = 15$.

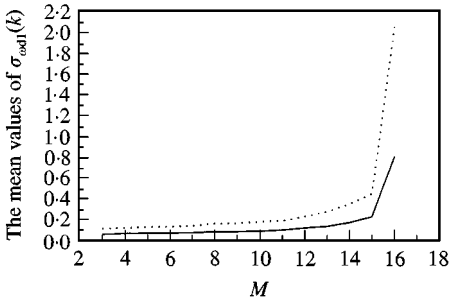

Figure 9. Mean values of standard deviation values of the estimated pseudo-damped natural frequencies when M varies: ——, mean values of $\sigma_{\omega_{d1}(k)}$; ……, mean values of $\sigma_{\omega_{d2}(k)}$.

where $\omega_{d1l}(k)$ denotes the lth estimate and $\bar{\omega}_{d1}(k)$ the mean of the L estimates. The influence of different choices of M is shown in Figures 8 and 9. Figure 8 displays $\sigma_{\omega_{d1}(k)}$ versus time for three different M's. Figure 9 gives the mean values of $\omega_{d1l}(k)$ and $\omega_{d2l}(k)$ when M varies from 3 to 16. In the simulations, SNR = 100 was used. It is noted that, when M is close to N, the estimation accuracy deteriorates drastically. When M is small, the standard deviations of $\sigma_{\omega_{d1}(k)}$ become smaller which indicates

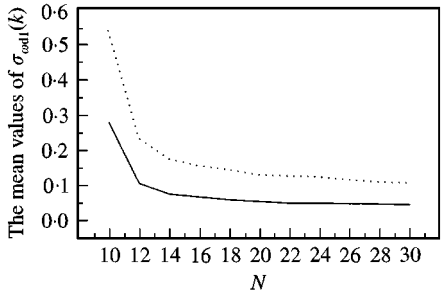

Figure 10. Mean values of standard deviation values of the estimated pseudo-damped natural frequencies when N varies: ——, mean values of $\sigma_{\omega_{d1}(k)}$; ....., mean values of $\sigma_{\omega_{d2}(k)}$.

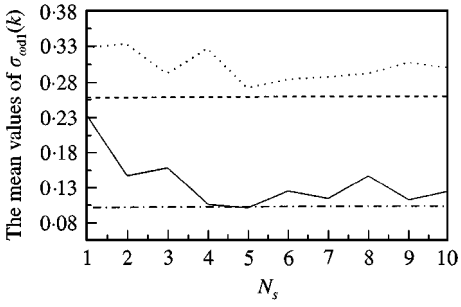

Figure 11. Mean values of standard deviation values of the estimated pseudo-damped natural frequencies when the number of sinusoidal terms varies: ——, mean values of $\sigma_{\omega_{d1}(k)}$ when the input is a series of sinusoidal terms; ....., mean values of $\sigma_{\omega_{d2}(k)}$ when the input is a series of sinusoidal terms; – · – · – · –, mean values of $\sigma_{\omega_{d1}(k)}$ when the input is white noise; – – – – – –, mean values of $\sigma_{\omega_{d2}(k)}$ when the input is white noise.

a better estimate. After M is below a certain value, a further reduction of M does not alter the standard deviations of $\sigma_{\omega_{d1}(k)}$ significantly. The effect of different N's is illustrated by Figure 10. It shows the mean values of $\sigma_{\omega_{d1}(k)}$ and $\sigma_{\omega_{d2}(k)}$ when $M = 5$ and $\mathrm{SNR} = 100$ were used. As expected, an increase of the experiment number–improves the estimation accuracy. The mean values of $\sigma_{\omega_{d1}(k)}$ and $\sigma_{\omega_{d2}(k)}$ increase significantly after $N = 12$. This indicates that there is a threshold value after which the estimate accuracy deteriorates drastically.

The case of using sinusoidal inputs was also tested. A torque was generated using

$$q_1(t) = 0{\cdot}1 \sum_{i=1}^{N_s} \sin(\omega_i t), \tag{47}$$

where ω_i is uniformly distributed in a range of $2 \leqslant \omega_i \leqslant 25$ rad/s and N_s is the total number of sinusoidal terms. One of questions is: how does the number of sinusoidal terms affect the estimation accuracy? Figure 11 shows the mean values of $\sigma_{\omega_{d1}(k)}$ and $\sigma_{\omega_{d2}(k)}$ versus N_s. The figure also gives the mean values of $\sigma_{d1}(k)$ and $\sigma_{d2}(k)$ when the white noise series were used as inputs. It is noted that, when the number of sinusoidal terms is small the quality of the estimates is poor. However, after N_s is

greater than a certain value, the quality of the estimates remains similar. In general, the white noise excitation results in a better estimate. The algorithm was tested against other conditions, such as, different available responses, noisy inputs and different moving patterns of the sliding masses. Due to limit of the paper length, they are not reported here.

5. CONCLUSIONS

This study has achieved two tasks: (1) to extend the well-defined modal concepts to characterize the dynamics of LTV system and (2) to further develop the previously proposed algorithm to identify LTV systems using the forced responses. For the first task, a discrete-time state-space model has been used to represent LTV systems. The eigenvalues of the discrete-time state transition matrix are related to the pseudo-modal parameters in analogy to LTI systems. The paper has explored how the pseudo-modal parameters can be used to describe the global properties of LTV systems. It is shown that the pseudo-modal parameters preserve certain characteristics of the conventional modal parameters defined for LTI systems.

For the second task, the paper has shown that the input and output Hankel matrices formed by an ensemble of data satisfy a matrix factorization equation. The key to the proposed method would be to modify the input matrix such that the part of the responses that does not emanate from the state is eliminated. With the modified output matrices, the previously developed algorithm can be readily implemented. A robotic manipulator with varying inertia links has been used as an example. The first part of the simulation has illustrated how the pseudo-modal parameters can help understand the dynamics due to different moving patterns of sliding masses. The second part of the simulation has tested the proposed identification algorithm. The results have indicated that the algorithm is capable of tracking the system variation and has a satisfactory robustness when the measurement noise is low or moderate. The simulation has also addressed several important issues such as selection of the parameters of the estimate model and exciting functions.

ACKNOWLEDGMENT

The support for this research provided by the National Science and Engineering Research Council of Canada under grant No. OGP-0184068 is gratefully acknowledged.

REFERENCES

1. N. M. M. Maia and J. M. M. Silva 1997 *Theoretical and Experimental Modal Analysis.* New York: John Wiley & Sons Inc.
2. L. A. Zadeh 1950 *Proceedings of the Institute of Radio Engineers* **38**, 291–299. Frequency analysis of variable networks.
3. L. A. Zadeh 1961 *Proceedings of the Institute of Radio Engineers* **49**, 1488–1503. Time-varying networks, I.

4. H. D'ANGLO 1970 *Linear Time-Varying Systems: Analysis and Synthesis*. Boston: Allyn and Bacon.
5. N. N. BOGOLIUBOV and Y. A. MITROPOLSKY 1961 *Asymptotic Methods in the Theory of Non-linear Oscillations*. Delhi: Hindustan Publishing Corp.
6. A. I. MAHYUDDIN and A. MIDHA 1994 *Transactions of the ASME, Journal of Mechanical Design* **116**, 298–305. Influence of varying cam profile and follower motion event types on parametric vibration and stability of flexible cam-follower systems.
7. M. BASSEVILLE, A. BENVENISTE, G. MOUSTAKIDES and A. ROUGEE 1987 *Automatica* **23**(4), 479–489. Detection and diagnosis of changes in the eigenstructure of nonstationary multivariable systems.
8. J. KONG and W. L. CLEGHORN 1988 *Proceedings of CSME Forum* **4**, 454–460. Finite element analysis of slider crank elastic mechanisms.
9. LIU, K. 1997 *Journal of Sound and Vibration* **204**, 487–505. Identification of linear time-varying systems.
10. J. B. ALLEN and L. R. RABINER 1997 *Proceedings of the IEEE* **65**, 1558–1564. A unified approach to short-time Fourier analysis and synthesis.
11. A. BENVENTISTE 1987 *International Journal of Adaptive Control and Signal Processing* **1**, 3–29. Design of adaptive algorithms for the tracking of time-varying systems.
12. Y. GRENIER 1983 *IEEE Transaction on Acoustics, Speech, and Signal Processing* **31**, 889–911. Time-dependent ARMA modelling of nonstationary signals.
13. M. NIEDZWIECKI 1990 *IEEE Transaction on Automation and Control* **35**, 610–616. Recursive functional series modelling estimators for identification of time-varying plants—more bad news than good.
14. J. B. MACNEIL, R. E. KEARNEY and I. W. HUNTER 1992 *IEEE Transaction on Biomedical Engineering* **39**, 1213–1225. Identification of time-varying biological systems from ensemble data.
15. M. VERHAEGEN and X. YU 1995 *Automatica* **31**, 201–216. A class of subspace model identification algorithms to identify periodically and arbitrarily time-varying systems.
16. M. VIBERG 1995 *Automatica* **31**, 1835–1851. Subspace-based methods for the identification of linear time-invariant systems.
17. S. SHOKOOHI and L. SILVERMAN 1987 *Automatica* **20**, 59–67. Linear time-variable systems: stability of reduced models.
18. S. M. SHAHRUZ and C. A. TAN 1989 *Journal of Sound and Vibration* **131**, 239–247. Response of linear slowly varying systems under external excitations.
19. G. H. GOLUB and C. F. VAN LOAN 1989 *Matrix Computations*. Baltimore, MD: The Johns Hopkins University Press.
20. G. JUMARIE 1988 *Robotica* **6**, 197–202. Trajectory control of manipulators with time varying inertia links.